nature communications

Article

https://doi.org/10.1038/s41467-025-60276-5

# Latent EBV enhances the efficacy of anti-CD3 mAb in Type 1 diabetes

Received: 13 June 2023

Accepted: 20 May 2025

Published online: 30 May 2025

Check for updates

Ana Lledó-Delgado[1], Paula Preston-Hurlburt[1], Lauren Higdon[2], Alex Hu[3], Eddie James[3], Noha Lim[2], S. Alice Long[3], James McNamara[4], Hai Nguyen[3], Elisavet Serti[2], Tomokazu S. Sumida[5] & Kevan C. Herold[1]

Teplizumab is approved for delaying the diagnosis of type 1 diabetes by modulating progression of disease. Compared to EBV-seronegative patients, those who are EBV-seropositive prior to treatment have a more robust response to teplizumab in two clinical trials. Here we compare the phenotypes, transcriptomes and development of peripheral blood cells before and after teplizumab treatment in participants. Higher number of regulatory T cells and partially exhausted CD8$^+$ T cells are found in EBV-seropositive individuals than in EBV-seronegative controls at the baseline in the TN10 and AbATE trials. Mechanistically, single cell transcriptomics and functional assays identify the downregulation of NFκB and T cell activation pathways after treatment in EBV-seropositive patients; among diabetes antigen-specific CD8$^+$ T cells, T cell receptor and mTOR signaling are also reduced. In parallel, signaling impairment is greater in adaptive than innate immune cells following teplizumab treatment in EBV-seropositive individuals. Our data thus indicate that EBV can impair signaling pathways in immune cells to modulate their responses in the context of type 1 diabetes.

Teplizumab, the FcR non-binding humanized anti-CD3 mAb is the first biologic approved for delay of type 1 diabetes (T1D) in patients at risk for clinical disease, and multiple trials have shown that treatment can modulate progression of new onset disease[1,2]. Despite its significance, clinical responses to teplizumab are varied and there is little known about the determinants of these responses. Latent viruses, such as Epstein Barr virus (EBV) and Cytomegalovirus (CMV) may modify human immune cells and are postulated to play a role in autoimmunity. It has been suggested that they have direct causative roles in some autoimmune diseases such as multiple sclerosis (MS), rheumatoid arthritis (RA), systemic lupus erythematosus (SLE), Sjogren's syndrome, and potentially others[3–7], but the ways in which it affects these diseases is not understood. In SLE, EBV-seropositive patients exhibit a higher frequency of EBV specific CD69$^+$ CD4$^+$ IFNγ producing T cells after EBV stimulation and there is an increased frequency of CD8$^+$ EBV reactive T cells[5]. Notably, most MS patients have prior exposure to EBV and EBV seroconversion associates with the onset of MS[3]. The risk of MS increased 32-fold after infection with EBV, but remained unaffected after infection with other viruses, including CMV. Furthermore, the discovery of cross-reactivity between antibodies targeting Epstein–Barr nuclear antigen 1 (EBNA1) and the central nervous system protein glial cell adhesion molecule in MS patients underscores the complex and intricate relationship between EBV and the pathology of MS[8]. Some have proposed treatment of MS with EBV reactive T cells to eliminate infected B cells[9].

Infectious agents may also suppress allergic and autoimmune responses. The inverse relationships between childhood illnesses and autoimmune diseases is striking and is the basis for the hygiene hypothesis[10,11]. Identifying the effects of EBV and CMV on human autoimmune responses has been challenging since cause and effect

[1]Department of Immunobiology, Yale University School of Medicine, New Haven, CT, USA. [2]Immune Tolerance Network, Bethesda, MD 20814, USA. [3]Center for Translational Immunology, Benaroya Research Institute at Virginia Mason, Seattle, WA, USA. [4]Autoimmunity and Mucosal Immunology Branch, Division of Allergy, Immunology and Transplantation, National Institute of Allergy and Infectious Diseases, National Institutes of Health, Bethesda, MD, USA. [5]Department of Neurology, Yale University School of Medicine, New Haven, CT, USA. e-mail: Kevan.herold@yale.edu

cannot be clearly established and many patients have already been exposed to these viruses by the time they present with autoimmunity. Model systems in which direct relationships between latent viruses and immune responses can be identified are limited since human EBV does not infect mice, and mice that can be infected with counterparts do not develop autoimmune diseases spontaneously.

Previous investigations of the mechanisms of action of teplizumab have shown that the drug caused a partial-exhaustion signature in $CD8^+$ T cells characterized by an increased frequency of $CD8^+$ cells expressing the transcription factor EOMES, and KLRG1 and TIGIT[12–14]. Comparisons of responses to biologics, in patients with and without latent EBV, CMV and other viruses, can give insights into their immune effects and the biologics in ways that are not possible with observational studies. Combined data from clinical trials of anti-CD3 mAb gave us the opportunity to understand the role of latent viruses on human immune responses, since among the participants in the studies, the majority of whom were children, only about half had previously been exposed to EBV and a smaller proportion to CMV.

Therefore, to understand how these viruses affect human immune responses we compare them in patients who had or had not previously been infected with EBV who were treated with teplizumab in two independent clinical studies. We identify changes in $CD4^+$, Tregs, and $CD8^+$ T cells in EBV-seropositive vs seronegative individuals at the baseline and more robust clinical responses to teplizumab in the seropositive study participants. Antigen receptor signaling pathways are reduced in T and B cells in EBV-seropositive individuals and the induction of T cell exhaustion is enhanced by teplizumab. Among diabetes antigen specific T cells, we also find reduced activation pathways even 18 months after drug treatment in EBV-seropositive participants. Collectively, these findings before and after treatment with teplizumab suggest a pervasive effect of EBV on adaptive immune cells that can modulate responses to the biologic treatment, teplizumab. The significance of latent EBV on clinical outcomes, such as autoimmunity, may vary by the cells engaged in the disease specific responses.

## Results

### Differences in multiple immune cell subsets associated with EBV serostatus

To identify the effects of prior exposure to EBV or CMV on immune cells, we compared the phenotypes of cells from the peripheral blood (PBMCs) of the 76 participants who were at high risk for development of clinical T1D in the TN10 trial, and 75 participants recently diagnosed with T1D in the AbATE trial, two clinical studies of teplizumab. The TN10 trial evaluated the time from treatment, with a single 14-day course of teplizumab vs placebo, until the diagnosis with clinical Stage 3 T1D in patients with Stage 2 T1D (i.e. 2 or more autoantibodies in blood and dysglycemia prior to clinical diagnosis). Of the 76 participants, 45% were EBV-seropositive (16/32 in the placebo and 18/44 in the teplizumab) when they enrolled in the trial. None had active EBV infection. The AbATE trial evaluated the effects of two of 14-day courses of teplizumab on stimulated C-peptide responses at 2 years in patients who were treated soon after the diagnosis with clinical T1D. At enrollment, 35% were EBV-seropositive (8/23 in the control and 18/52 in teplizumab arms) (Table 1) and none had active EBV infection. The PBMCs were analyzed with 260 parameters comparing the frequency and intensity of expression of markers on T, Tregs, NK and NKT cells between EBV-seropositive and seronegative participants (Supplementary Data 1, gating in ref.[14] and Supplementary Fig. 1). We found significant differences in the expression of 10 markers on $CD8^+$, $CD4^+$ T cells and Tregs after FDR correction ($p < 0.001$). (Supplementary Data 1 and Fig. 1A).

The co-infection with CMV, another common latent virus may have affected the phenotypes of the cells. When we compared participants who were CMV seropositive or negative, without regard to EBV serostatus, we found differences in CD8 + , CD4 + , and NKT cells following FDR correction. In CMV seronegative participants, there were increased numbers of $CCR7^+$ $CD45RA^+$ and $PD1^+$ TEMRA $CD8^+$ T cells. Conversely, in $CD4^+$ T cells, CMV seropositive individuals showed higher levels of CD57+ effector memory (EM), $CD57^+$ TEMRA, and $CD57^+$ $KLRG1^+$ $PD1^+$ cells, whereas CMV seronegative participants had a higher proportion of EM cells Supplementary Fig. 2). There were 36 markers that were significantly different ($p < 0.05$) when we compared the participants who were EBV-seropositive only ($n = 22$) to those who were EBV and CMV seropositive ($n = 12$) (Supplementary Data 2) but none of these markers met statistical significance after correction for multiple comparisons.

To further understand these differences among immune cell subsets in the EBV-seropositive and seronegative individuals, we compared transcriptional profiles of PBMCs by single-cell RNA-seq (scRNAseq) with 10X Chromium 3′ sequencing platform. We annotated six major clusters based on the expression of key identity genes: $CD8^+$ T cells (*CD8A*$^{hi}$, *CD3D*$^{hi}$, *CD3E*$^{hi}$), $CD4^+$ T cells (*CD8A*$^-$, *CD3D*$^{hi}$, *CD3E*$^{hi}$), B cells (*CD79A*$^{hi}$, *MS4A1*$^{hi}$), monocytes (*CD14*$^{hi}$, *FCGR3A*$^{hi}$) dendritic (*PLD4*$^{hi}$, *LILRA4*$^{hi}$) and platelets (*CD3*$^-$ *PPBP*$^+$) (Fig. 1B and Supplementary Fig. 3). The distribution of cells was similar across donors (Supplementary Fig. 4). However, we found significant differences in the major cell subsets based on the EBV serological status. There were 57, 41, 34, 123 and 2 genes that were differentially expressed (DEGs) in the $CD4^+$, $CD8^+$, B cells, monocytes, and dendritic cells at the baseline (Fig. 1C and Supplementary Data 3–7). (We did not find DEGs, after FDR correction, in NK cells at the baseline in the EBV-seropositive and seronegative participants). Figure 1D shows pathways that were differentially enriched using IPA analysis (Supplementary Data 8–11). Consistent with our findings by flow cytometry, in $CD8^+$ T cells, there was a prediction of activation of pathways related to exhaustion (increased CTLA4 signaling in $CD8^+$ T cells ($p < 0.0001$) and reduced expression of genes in antigen receptor signaling among $CD4^+$, $CD8^+$ T, and B cells. (e.g. PI3K signaling in B cells ($p < 0.0001$), protein kinase A signaling in $CD4^+$, $CD8^+$ and B cells ($p = 0.0001$, $p = 0.0001$,$p = 0.0002$), NFκB signaling in $CD8^+$ T cells and B cells ($p = 0.0003$ and $p = 0.014$), mTOR signaling in $CD4^+$ T cells ($p = 0.024$) and others.

Among B cells, there were significant differences in B cell receptor and ERK/MAPK signaling. To validate this finding, we compared ERK phosphorylation in B cells from a separate group of EBV-seropositive or seronegative individuals with T1D. Following IgM cross-linking, there was higher levels of ERK phosphorylation in 6 EBV-seronegative vs 5 EBV-seropositive donors ($p = 0.04$) (Fig. 1E and Supplementary Fig. 5).

**Table 1 | Baseline characteristics of clinical trial participants**

| Trial | Treatment arm (n) | Age (yrs, median (25th and 75th percentile) | EBV-seropositive (n, %) | CMV seropositive (n, %) |
|---|---|---|---|---|
| TN10 | Teplizumab (44) | 14.6 (11.5, 22.8) | 18, 41% | 10, 23% |
| | Placebo (32) | 13.5 (10.8, 17.2) | 16, 50% | 7, 22% |
| ITN027AI (AbATE) | Teplizumab (52) | 11.8 (10.4,14.8) | 18 (35%) | 13 (25%) |
| | Control (23) | 12.0 (9.86, 15.7) | 8 (35%) | 4 (17%) |

https://doi.org/10.1038/s41467-025-60276-5

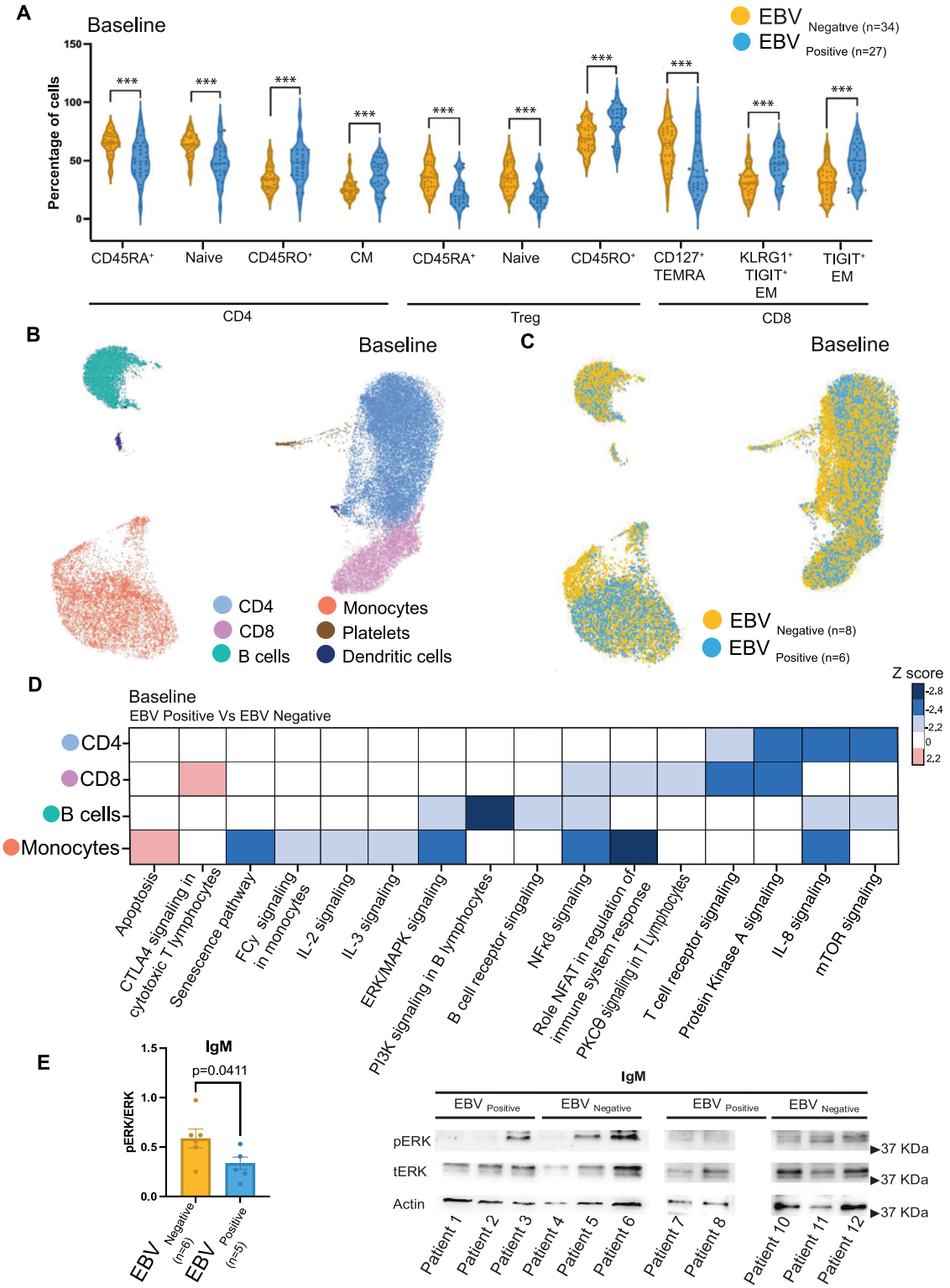


## EBV-seropositive patients have improved clinical responses to teplizumab treatment

These findings ex vivo distinguished phenotypic and transcriptional differences in cell subsets among EBV-seropositive and seronegative individuals that may affect their functional responses in vivo. We therefore compared the clinical responses to teplizumab treatment in the two clinical studies based on EBV serostatus at the time of drug treatment.

The patients were followed for a median of 80.5 months. Among the patients with Stage 2 T1D who were EBV-seropositive (Table 1) the median time to diagnosis with Stage 3 T1D was delayed significantly with teplizumab treatment (35.5 months in placebo vs 86.9 months in teplizumab- difference of 51.4 months, Logrank: $p = 0.008$, 0.045 after Sidak's adjustment, Fig. 2A). In the EBV-seronegative participants, there was a numerical delay in the median time to diagnosis with Stage 3 T1D, but the difference was not statistically significant (12 months (placebo $n = 16$) vs 38 months (teplizumab $n = 16$, $p = 0.1555$, 0.635 after Sidak´s adjustment)). There was a difference of 48.9 months in the time to diagnosis in the EBV-seropositive and seronegative participants (86.9 vs 38 months $p = 0.127$, 0.557 with Sidak's adjustment) in

**Fig. 1 | Changes in immune cell subsets at the baseline among EBV positive or negative individuals. A**Violin plots showing the percentages of populations from the TN10 trial analyzed by flow cytometry and found to be significantly different after FDR correction. Colors identify EBV serological status($n = 27$ EBV-seropositive (blue), $n = 34$ EBV-seronegative (yellow)) (unpaired t tests between EBV positive and EBV negative participants with a two stage linear step up following Benjamin, Krieger and Yekutieli to correct for false discovery rate (FDR) from multiple hypothesis testing, ***$p$ values = 0.0002, 0.00002, 0.0003, 0.0001, 0.00002, 0.00001, 0.0001, 0.00004, 0.0001, 0.0001 in order from left to right in the violin plots, see Supplementary Data 1). **B** UMAP visualization of the clusters at the baseline. Points represent individual cells and color denote cluster classification as labeled ($n = 6$ EBV-seropositive (blue) and $n = 8$ EBV-seronegative (yellow)). **C** UMAP visualization of the cells at the baseline. Points represent individual cells and color denote EBV serological status ($n = 6$ EBV-seropositive and $n = 8$ EBV-seronegative). **D** Heatmap showing the Z score of the significant pathways ($p < 0.05$ after FDR correction) in the major clusters at the baseline ($n = 6$ EBV-seropositive and $n = 8$ EBV-seronegative). Pathways were inferred based on the DEGs between EBV positive and EBV negative in each cell subset using IPA software. Blue and red scale denote grades of prediction of downregulation or upregulation of the pathways based on the Z score. **E** Western blot showing phosphorylation of ERK in B cells after stimulation with anti-human IgM. The ratio of pERK/totalERK was corrected for loading (actin). The levels of pERK are decreased in the EBV-seropositive ($n = 6$) vs EBV-seronegative ($n = 5$) individuals (mean values ± SEM, Student's $t$-test, *$p = 0.04$). CM: central memory; TEMRA: T effector memory RA; EM: effector memory. Source data are provided in the Source Data file.

the teplizumab group. In the EBV-seropositive patients ($n = 34$) there was a greater frequency of diagnosed Stage 3 diabetes among the placebo-treated patients (41.2% $n = 14$) compared to the teplizumab-treated patients (26.5%, $n = 9$) (Fisher's exact test $p = 0.03$). In the EBV-seronegative patients ($n = 42$), at the end of the observation period, 19 of the placebo treated patients (45.2%) and 14 of the teplizumab treated patients (33.3%) were diagnosed with Stage 3 T1D (Fisher's exact test $p = 0.44$). Among patients who were EBV-seropositive at study entry ($n = 34$), 8 of those in the teplizumab group had detectable viral loads at weeks 3-6, that cleared spontaneously. The responses to teplizumab were not statistically different between the EBV-seropositive, teplizumab treated patients, with and without detectable EBV viral loads after treatment.

A smaller proportion of the TN10 trial participants, 25% ($n = 10$) in the teplizumab group and 21.8% ($n = 7$) in the placebo group, were CMV seropositive (Table 1), but the effects of CMV serostatus were the opposite of EBV. Teplizumab treatment did not show a significant delay in the time to Stage 3 T1D in the CMV seropositive patients (24.6 months for placebo, $n = 7$, vs 39.7 months for teplizumab, $n = 10$, $p = 1.00$ after Sidak's adjustment), but showed significant delay in the CMV seronegative patients (30 months for placebo ($n = 25$) vs 59.9 months for teplizumab ($n = 34$) $p = 0.0062$ after Sidak's adjustment) (Supplementary Fig. 6A).

In the TN10 trial, the small number of participants who were CMV seropositive and either EBV-seronegative or EBV-seropositive ($n = 5$ and $n = 12$) limited our ability to assess the effects of CMV serostatus on the response to teplizumab in these subgroups. The median time to diagnosis with Stage 3 T1D was longer in the EBV-seropositive participants, who were treated with teplizumab, whether they were CMV seropositive (83 months in EBV-seropositive ($n = 83$) vs 21 months in EBV-seronegative ($n = 3$)), or CMV seronegative (127 months in EBV-seropositive ($n = 11$) vs 47 months in EBV-seronegative ($n = 23$)).

We confirmed these clinical findings in a second trial that evaluated the effects of teplizumab on stimulated C-peptide responses, over 2 years, in patients who had new onset clinical (Stage 3) T1D, (ITN027AI, AbATE) (Table 1). There was a strong correlation between age in quartiles and EBV seropositivity (R = 0.99 TN10 trial R = 0.83 AbATE trial). When we corrected the C-peptide levels for age and baseline levels, teplizumab treatment resulted in improved stimulated C-peptide levels (vs control) in both the EBV-seronegative (difference of least means square (LSMs (95%CI)) −0.1125, (−0.197, −0.0277), $p = 0.0096$) and EBV-seropositive participants (difference of LSMs = −0.178 (−0.293, −0.064), $p = 0.0024$), but the C-peptide levels were significantly greater in the EBV-seropositive vs EBV-seronegative teplizumab-treated individuals (difference of LSMs = −0.081 (−0.161, −0.0003), $p = 0.049$) (Fig. 2B). In the AbATE trial, there were 17 patients who were CMV seropositive (13 teplizumab-treated and 4 controls). We did not find a significant difference in the C-peptide levels between the CMV seronegative and seropositive participants who were treated with teplizumab (difference of LSMs=0.013 (−0.078, 0.104), $p = 0.78$) (Supplementary Fig. 6B). Even when we corrected the C-peptide AUC among the EBV-seropositive vs seronegative participants for their CMV serostatus, we found a consistent difference in the C-peptide response in the EBV-seronegative vs seropositive participants (difference of LSMs −0.083 (−0.165, −0.0008), $p = 0.048$) (Supplementary Fig. 6C).

## EBV-seropositive patients have increased expression of markers of partial exhaustion phenotype on CD8$^{+\pm}$ T cells with teplizumab treatment

Teplizumab was previously shown to induce markers of partial exhaustion of CD8 + T cells characterized by an increase in the expression of EOMES$^+$ and frequency of KLRG1$^+$TIGIT$^+$ CD8$^+$ cell[12,13]. We compared, by flow cytometry, EOMES expression and the frequency of these cells over time after teplizumab treatment in the two trials. In the TN10 trial, there was a higher proportion of EOMES$^+$ CD8$^+$ central memory (CM) cells in the EBV-seropositive vs seronegative teplizumab treated patients that was not seen for the placebo treated patients (difference of LSMs (95%CI) 11.7(19.64, 3.9), $p = 0.004$ and difference of LSMs 6.28(16.0, −3.45) $p = 0.20$ respectively, $n = 64$). Consistent with these results, there was increased gene expression of EOMES in CD8$^+$ T cells ($n$=4 EBV-seropositive, $n$=3 EBV-seronegative, Supplementary Figure 7A-C). There was a significant difference in the EOMES$^+$CD8$^+$ CM cells in the teplizumab vs placebo in the EBV-seropositive patients (difference of LSMs 11.21, (1.95, 20.5) $p = 0.018$) but not in the EBV-seronegative patients (difference of LSMs 5.73, (−2.7, 14.2) $p = 0.182$) (Fig. 3A). Moreover, the frequency of EOMES$^+$ CD8$^+$(difference of LSMs 7.46, 95%CI= (12.5, 2.42), $p = 0.004$, $n = 58$), was higher in EBV-seropositive vs EBV-seronegative in the teplizumab group in the AbATE trial (Fig. 3B). We found similar differences in KLRG1$^+$TIGIT$^+$ CD8$^+$ effector memory (EM) and central memory (CM) T cells in EBV-seropositive and EBV-seronegative participants who were treated with teplizumab (difference of LSMs (95% CI)26.5 (34.2, 18.8), $p < 0.0001$, difference of LSMs 16.6 (23.3, 9.9), $p < 0.0001$ respectively) in the TN10 trial (Fig. 3C-D). These differences were unlikely to be explained exclusively by an effect of teplizumab: the frequency of KLRG1$^+$TIGIT$^+$ CD8$^+$ CM cells was higher in the EBV-seropositive patients treated with teplizumab vs EBV-seropositive patients treated with placebo (difference of LSMs 12.8(20.7, 5), $p = 0.0016$) but not in the EBV-seronegative patients treated with teplizumab vs placebo (difference of LSMs 3.6 (10.7, −3.47), $p = 0.312$) (Fig. 3D). Similarly, among the KLRG1$^+$TIGIT$^+$CD8$^+$ EM cells, there was a significant difference with teplizumab treatment in the EBV-seropositive patients in comparison with the EBV-seropositive patients treated with placebo (difference of LSMs 10.7(19.76, 1.68), $p = 0.02$) but not in the EBV-seronegative (difference of LSMs 0.57 (8.78, −7.63), $p = 0.89$) patients. In the AbATE trial there was a significant difference in the frequency of the KLRG1$^+$TIGIT$^+$ CD8$^+$ T cells in the teplizumab treated patients who were EBV-seropositive vs EBV-seronegative (difference of LSMs 5.7(10.7, 0.9), $p = 0.02$) (Fig. 3E).

https://doi.org/10.1038/s41467-025-60276-5

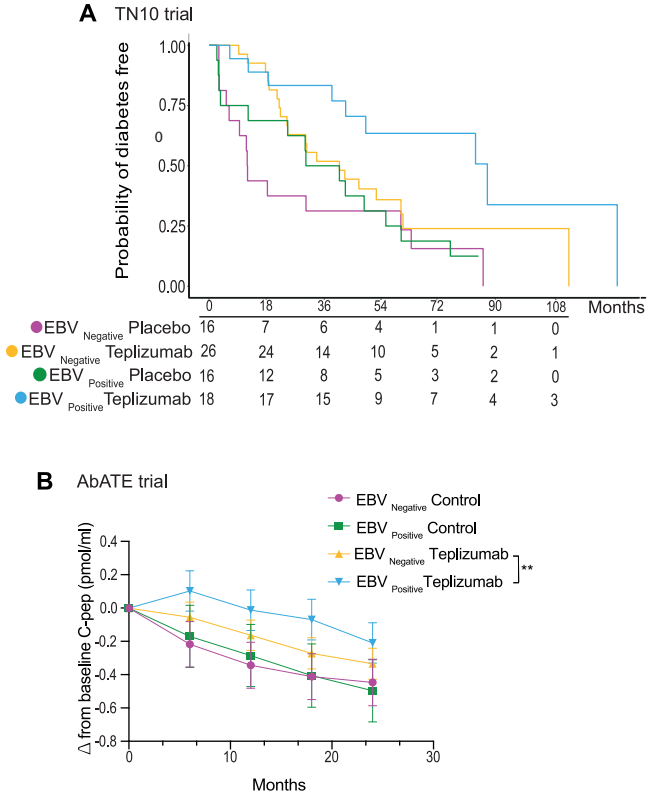


**Fig. 2 | Effects of EBV serostatus on clinical responses to teplizumab. A** Kaplan Meier curve showing the progression from Stage 2 T1D to Stage 3 T1D in TN10 study participants who were EBV-seropositive ($n = 18$, teplizumab (blue), $n = 16$ placebo (green)) or EBV-seronegative ($n = 26$ teplizumab (yellow), 16 placebo (magenta)) at enrollment. Median times to development of Stage 3 T1D: Placebo EBV-seronegative: 12 months; Placebo EBV-seropositive: 35.5 months; Teplizumab EBV-seronegative: 38 months; Teplizumab EBV-seropositive: 86.9 months (Logrank $p = 0.005$) (See text for subgroup comparisons). **B** In the AbATE trial (control: $n = 16$ EBV-seronegative (magenta), $n = 7$ EBV-seropositive (green), treatment: $n = 34$ EBV-seronegative (yellow), $n = 18$ EBV-seropositive (blue)). The data are the least square means of the lnC-peptide(AUC + 1) ( ± 95%CI), corrected for the baseline level and age, from the mixed model. (Control EBV-seronegative vs teplizumab EBV-seronegative (group difference of least square means (LSM, (95% CI): 0.111 (.063, 0.159) $p < 0.0001$), Control EBV-seropositive vs teplizumab EBV-seropositive (0.19(0.122, 0.258), $p < 0.0001$). Teplizumab EBV-seronegative vs teplizumab EBV-seropositive (0.066 (0.016, 0.11) $^{**}p = 0.008$). The annotated comparisons are between teplizumab treated participants who were EBV-seropositive vs EBV-seronegative. Source data are provided in the Source Data file.

## Interactions between EBV serostatus and teplizumab responses in patients

These findings, from two independent clinical trials of teplizumab, showed increased frequencies of $CD8^+$ T cells that are purported to mediate the biologic effects of the drug in the EBV-seropositive participants. However, our flow cytometry analysis indicated there were effects of EBV on other cells prior to teplizumab treatment. We therefore compared the changes in the frequency and transcriptomes of immune cells of 4 patients EBV-seropositive vs 3 patients EBV-seronegative over time after teplizumab treatment in the TN10 trial to identify how the effects on $CD8^+$ and other cells may contribute to the improved efficacy. The samples were obtained approximately 3 months (first visit) and 18-24 months (last visit) after study drug.

We did not find a significant difference in the frequencies of $CD8^+$, $CD4^+$ T cells, B cells, monocytes, or dendritic cells overall by flow cytometry or scRNAseq (Supplementary Fig. 8 and Supplementary Fig. 9 respectively). We further analyzed the cell subsets by scRNAseq using transcriptomic markers described in Supplementary Figs. 3, 4. There were trends of differences in the frequency of cell subsets but the differences in the number of cells did not reach statistical significance (Supplementary Fig. 9 A-D).

We performed pathway analyses (IPA) to compare gene expression between the teplizumab-treated EBV-seropositive and seronegative patients, at different timepoints in the cell subsets (Fig. 4 and Supplementary Data 12-17). There was reduced expression of genes in the NFκB and protein kinase A signaling pathways ($p = 0.0007$ and 0.00002 respectively) in $CD8^+$ T effector cells at the baseline of EBV-seropositive patients. In the $CD4^+$ Naive T cells, cAMP signaling ($p = 0.026$) and mTOR signaling ($p = 0.0002$) showed less enrichment in EBV positive at the baseline with absolute highest Z score. B cells also showed the same tendency with downregulation of pathways related to B cell receptor signaling and activation at the baseline (Fig. 1D). To identify the changes in pathways with treatment, at 3 and 18 months, we filtered out the DEGs between teplizumab and placebo at the baseline, and the pathways that were changed in the placebo group (Supplementary Fig. 10A). In the teplizumab treated-EBV-seropositive patients, NFκB pathway showed less enrichment at 3 and 18 months, compared to the teplizumab treated EBV-seronegative patients (Fig. 4B). In addition, in $CD8^+$ effector cells, pathways of cytokine signaling (STAT3 ($p = 0.00378$) as well as mTOR signaling ($p = 0.00455$) pathway gene expression were less enriched at 3 months (Fig. 4B and Supplementary Fig. 10B respectively, $p$ values in Supplementary Data 12) and 18 months (Fig. 4C). In both $CD8^+$ effector and memory T cells we found an enrichment of IFNγ signaling pathway at 3 months which we recently described as a consequence of teplizumab treatment, with no difference in enrichment between both groups at 18 months[15]. In the $CD4^+$ Tregs, we found downregulation of NFκB at 3 months (Fig. 4D) and 18 months (Supplementary Fig. 10C) in EBV-seropositive individuals. Among B cells, we found significant differences at the first and last visit in cytokine signaling pathways and in B cell receptor and ERK/MAPK signaling (Fig. 4E). These data suggest a downregulation of the pathways related to cytokine and activation signaling in EBV positive in comparison with EBV negative maintained under teplizumab treatment.

## Effects of EBV serostatus on autoantigen specific $CD8^+$ T cells

To determine whether the findings with the general subsets pertain to antigen specific T cells, we isolated $CD8^+$ T cells that were selected for binding to T1D autoantigens from PBMCs of TN10 trial participants using tetramer sorting and analyzed the transcriptome of each individual cell. We compared EBV-seropositive and EBV-seronegative patients in the treatment groups at the baseline ($n = 6$ EBV-seropositive and $n = 4$ EBV-seronegative) and at 18 months after teplizumab ($n = 3$ EBV-seropositive and $n = 3$ EBV-seronegative) (Supplementary Data 18).

At the baseline ($n = 4$, placebo, and $n = 6$, teplizumab), there were 773 DEGs between the cells from the EBV-seropositive vs EBV-seronegative patients. By IPA analysis there was a significant increase in IFNγ signaling (Z score=2.1, $p = 0.04$) but reduced Class I MHC antigen processing and presentation (Z score = −3.4, $p = 0.01$) (Fig. 5A). At 18 months, there were 1404 DEGs including increased expression of *EOMES* ($p = 0.009$) and *HLA-DRB1* ($p = 0.03$) in T1D specific $CD8^+$ T cells of EBV positive individuals compared to EBV negative at 18 months in the teplizumab group (Fig. 5C), as well as reduced expression of *IL1RAP, IFNAR1, IL27RA, IL32, JAK1* which are linked to immune activation (Supplementary Data 19), The TCR signaling (Z score = −3.3, $p = 0.006$), TNF signaling (Z score = −2.89, $p = 0.001$) and interferon alpha and beta signaling (Z score = −3.16, $p = 0.02$) pathways were reduced in T1D specific $CD8^+$ T cells from the EBV positive individuals 18 months after of teplizumab treatment (Figs. 5B, 5D-E and Supplementary Data 20). In addition, among the EBV-seropositive vs seronegative donors, there was reduced expression of *TCF7* (log2 fold

https://doi.org/10.1038/s41467-025-60276-5

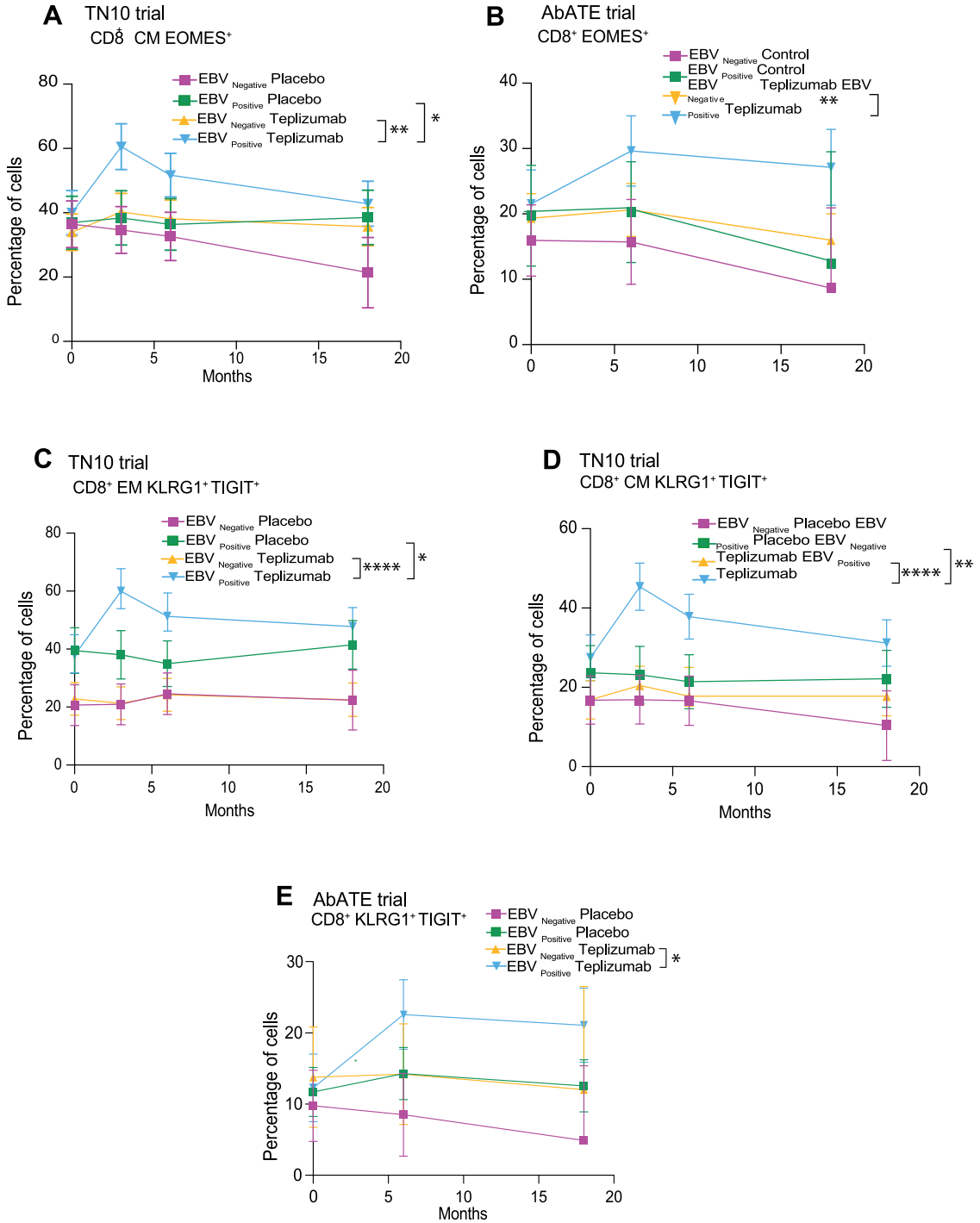


**Fig. 3 | Induction of partially exhausted phenotype CD8⁺ T cells with teplizumab in clinical trial participants. A** Frequency of CD8⁺ Eomesodermin (EOMES)⁺ T cells among CD8⁺ central memory (CM) T cells in the EBV-seropositive ($n = 16$) vs EBV-seronegative ($n = 22$) teplizumab treated in the TN10 trial by flow cytometry, (A, $^{**}p = 0.004$). **B** Frequency of CD8⁺EOMES⁺ T cells in the EBV-seropositive ($n = 10$) vs EBV-seronegative ($n = 18$) teplizumab treated in the AbATE trial by flow cytometry, ($^{**}p = 0.004$, $^{*}p = 0.01$). **C** Frequency of KLRG1⁺ TIGIT⁺ effector memory (EM) CD8⁺ T cells in the TN10 trial among EBV-seropositive ($n = 16$) vs EBV-seronegative ($n = 22$) participants by flow cytometry with teplizumab treatment ($^{****}p < 0.0001$, $^{*}p = 0.02$). **D** Frequency of KLRG1⁺ TIGIT⁺ CM CD8⁺ T cells in the EBV-seropositive (n = 16) vs EBV-seronegative ($n = 22$) participants by flow cytometry with teplizumab treatment ($^{****}p < 0.0001$, $^{*}p = 0.016$). **E** Frequency of KLRG1⁺TIGIT⁺ CD8⁺ T cells in the AbATE trial ($^{*}p = 0.02$). **A**–**E**, the data are the mean values +/− 95% CI from a mixed model for repeated measures without correction for the baseline or multiple comparisons. Control: EBV-seronegative: square magenta, EBV-seropositive: square green; Teplizumab EBV-seronegative triangle yellow, EBV-seropositive inverted triangle blue. The group comparisons are shown in the legends). Source data are provided in the Source Data file.

change = −0.0.757, $p$(adj)=0.036) (Fig. 5C). We compared EBV specific vs T1D specific T cells in EBV-seropositive donors with an enrichment in pathways related G2 pathway (p value = 0.01, ES = −0.89), proteosome ($p$ value = 0.01, ES = 1.6) and glycolysis ($p = 0.006$ ES = 1.3) (Supplementary Fig. 11).

## EBV serostatus modifies T cell differentiation

To understand how T cell development differed between EBV-seropositive and EBV-seronegative patients in the TN10 trial, we performed a pseudotime analysis comparing the trajectories of T cells from EBV-seropositive vs seronegative TN10 study participants treated

https://doi.org/10.1038/s41467-025-60276-5

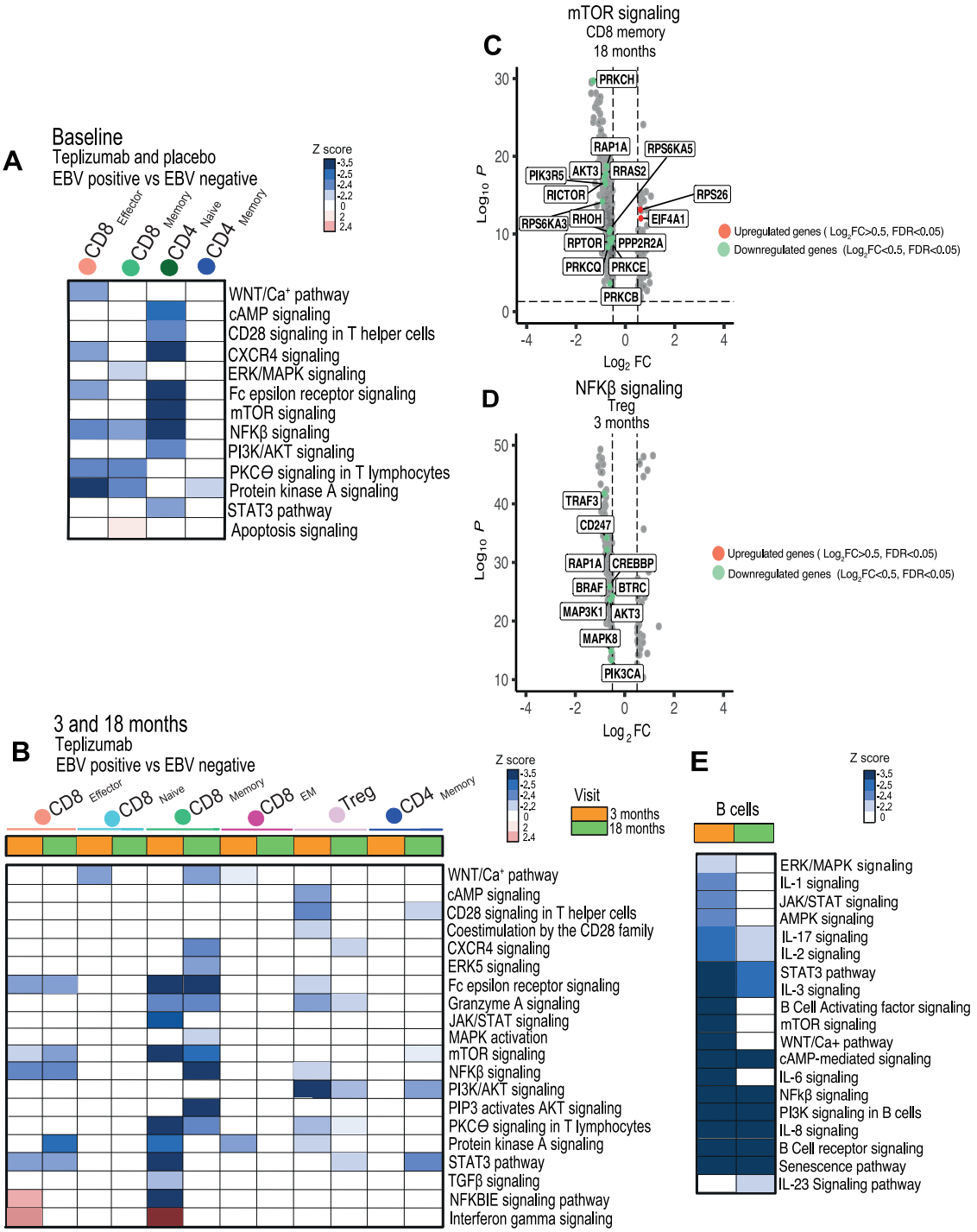


**Fig. 4 | Transcriptional changes and pathway analysis of cells from teplizumab treated patients in the TN10 trial who are EBV-seropositive vs EBV-seronegative. A** Heatmap showing the Z score of the pathways with significant differences in the $CD8^+$ and $CD4^+$ T cells subclusters at the baseline ($n = 6$ EBV-seropositive and $n = 8$ EBV-seronegative). The pathways were determined by IPA analysis based on the DEGs between EBV positive and EBV negative in the placebo and teplizumab group. Blue and red scale denote grades of prediction of down-regulation or upregulation of the pathways based on the Z score. **B** Heatmap showing the Z score of the pathways with significant differences (in the $CD8^+$, $CD4^+$ T cells at 3 months and 18 moths ($n = 4$ EBV-seropositive, $n = 3$ EBV-seronegative)). The pathways were determined by IPA analysis and based on the DEGs between EBV positive and EBV negative in the teplizumab group at each timepoint after filtering out the genes that showed changes at the baseline and pathways that change in the placebo group at the same timepoints. Blue and red scale denote grades of prediction of downregulation or upregulation of the pathways based on the Z score. **C** Volcano plot visualization of the DEGs in EBV positive vs negative related to the mTOR signaling pathway in the CD8 effector cluster at 18 months, and (**D**) Volcano plot visualization of the DEGs in EBV positive vs negative related to the NFκB in the Treg cluster at 3 months. **E** Heatmap showing the Z score of the significant pathways in the B cells cluster at 3 months and 18 months. CM: central memory, EM: effector memory.

https://doi.org/10.1038/s41467-025-60276-5

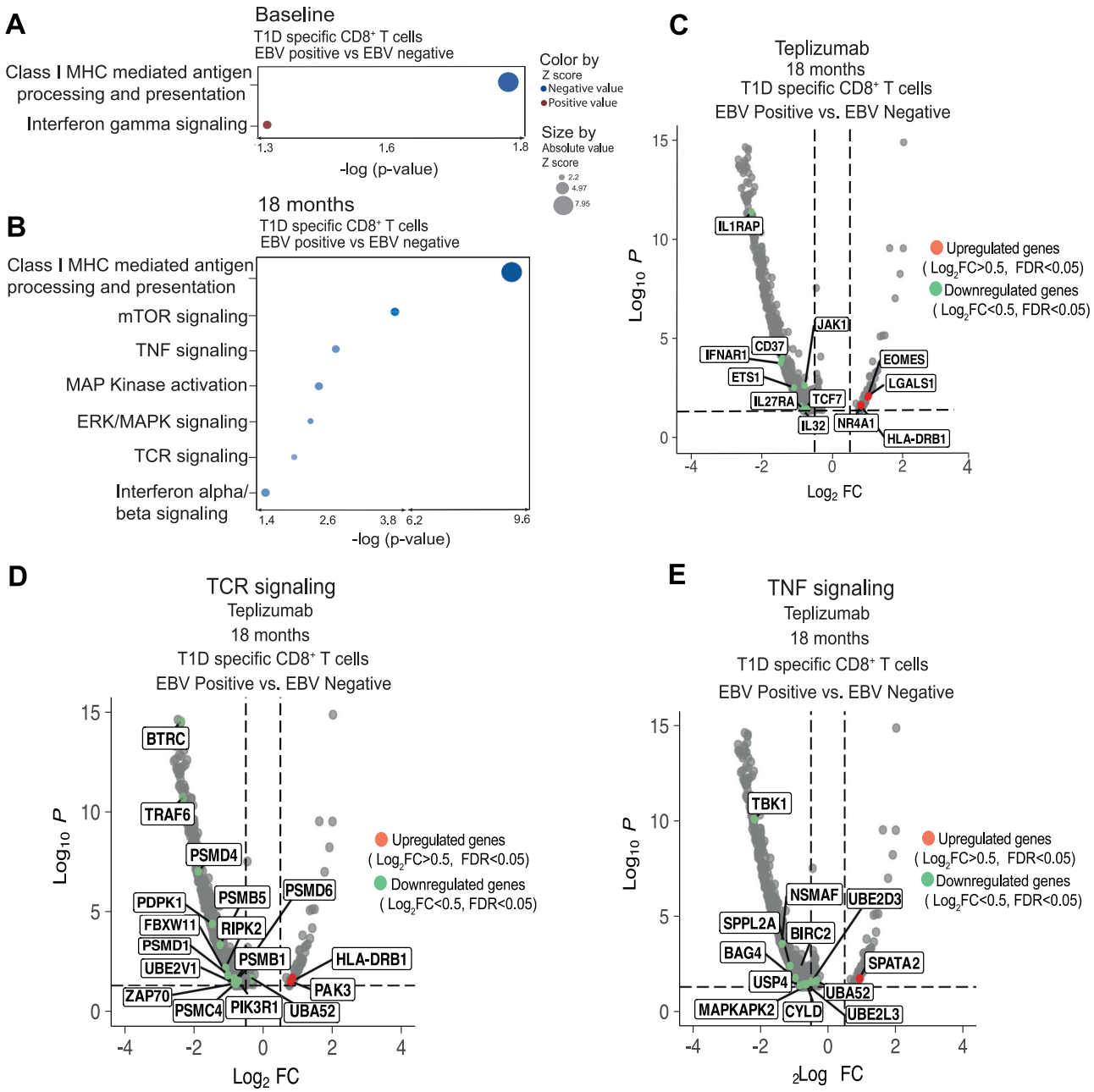


**Fig. 5 | Effects of EBV serostatus on autoantigen specific CD8⁺ T cells. A** Bubble plot showing the Z score and p values of the pathways with significant differences in the T1D specific CD8⁺ T cells at the baseline ($n = 4$ placebo, (EBV-seropositive=2 and EBV-seronegative=2), $n = 6$ teplizumab, (EBV-seropositive =4, EBV-seronegative =2)) (**B**) Bubble plot showing the Z score and p values at 18 months in the teplizumab group ($n = 3$ EBV-seropositive, $n = 3$ EBV-seronegative). The pathways were determined by IPA analysis based on the DEGs between EBV positive and EBV negative in the T1D specific CD8⁺ T cells of the teplizumab group filtering out the genes that also show a change at the baseline. Blue scale denotes grades of prediction of downregulation of the pathways based on the Z score. **C** Volcano plot visualization of the DEGs in the T1D specific CD8⁺ T cells between EBV-seropositive vs seronegative at eighteen months in the teplizumab group ($n = 3$ EBV-seropositive and $n = 3$ EBV-seronegative).Volcano plot visualization of the DEGs in EBV positive vs negative related to the TCR signaling pathway (**D**) and TNF signaling (**E**) in the T1D specific CD8⁺ T cells at 18 months.

with teplizumab. UMAPs were prepared to identify different states of cell differentiation that differed between the EBV-seropositive and seronegative patients (Fig. 6).

Pseudotime analysis, a computational and statistical technique commonly employed in scRNAseq, can elucidate the developmental or temporal trajectory of individual cells within a diverse population. This method aims to reconstruct the dynamic progression of cells along a continuous path, representing various biological processes such as development, responses to stimuli, or other temporal changes in gene expression[16].

There were differences in the trajectories of CD8⁺, CD4⁺ T and B cells between the EBV-seropositive and seronegative participants throughout the study and specifically at 18 months (Fig. 6, and Supplementary Figs. 12, 13 and 14). There was an increased in cells that determined the differentiation into CD8⁺ effector and effector memory cells in the EBV-seropositive individuals at the earlier stages of the pseudotime (Fig. 6A-B). Genes related to exhaustion pathways and inhibition of immune system (*IL10RA*⁺($p = 0.00003$), *TIGIT*⁺ ($p < 0.0001$), *LAG3*⁺($p < 0.0001$)) were overall enriched in the EBV-seropositive teplizumab and maintained at 18 months (Supplementary Fig. 12).

https://doi.org/10.1038/s41467-025-60276-5

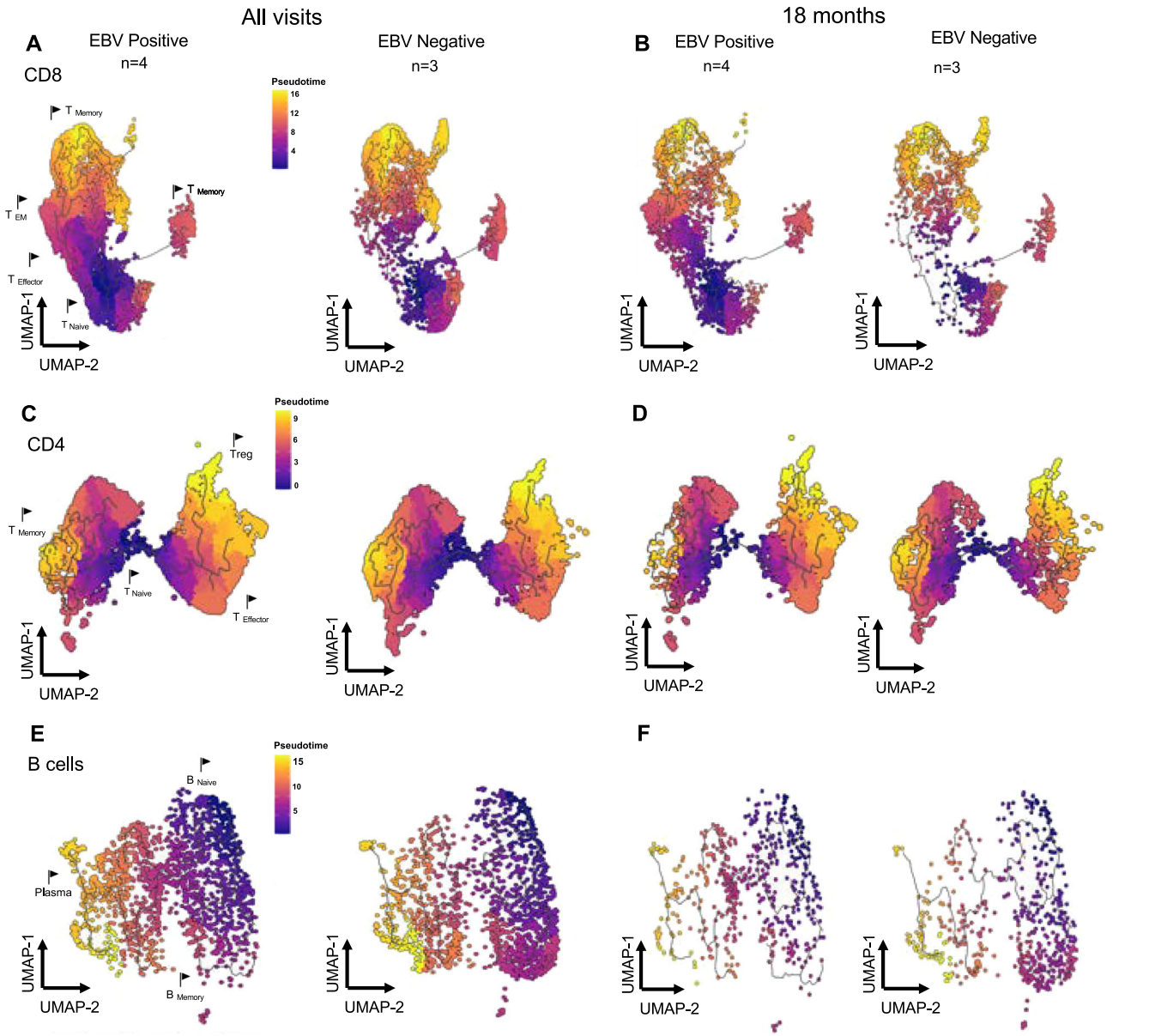


**Fig. 6 | Pseudotime analysis of CD8⁺, CD4⁺ and B cells in the TN10 trial.** UMAPs showing the pseudotime analysis of CD8⁺ T cells in the EBV-seropositive and EBV-seronegative in teplizumab treated participants (**A**) at all the visits and (**B**) at 18 months ($n = 4$ EBV-seropositive $n = 3$ EBV-seronegative). UMAPs showing the pseudotime analysis CD4⁺ T cells in the EBV-seropositive vs EBV-seronegative participants (**C**) at all the visits and (**D**) at 18 months ($n = 4$ EBV-seropositive $n = 3$ EBV-seronegative). UMAPs showing the different stages of differentiation of B cells in the EBV-seropositive and EBV-seronegative participants (**E**) at all the visits and (**F**) at 18 months ($n = 4$ EBV-seropositive $n = 3$ EBV-seronegative). Transcript dynamics are illustrated by the color of the pseudotime. The location of transcriptional signatures for the major cell states identified are indicated by markers on pseudotime visualizations ($T_{Memory}$, $T_{EM}$, $T_{Naive}$, $T_{Effector}$, Treg, $B_{Naive}$, Plasmablast, $B_{Memory}$).

In CD4⁺ T cells, the cells that differentiated into memory cells was reduced in the EBV-seropositive patients (Fig. 6C-D). *LEF1* was among the top differentially expressed gene in the CD4⁺ memory cells 18 months (Supplementary Data 21–26) from the EBV-seropositive vs seronegative patients. We found differences in the expression across the pseudotime in *LEF1* but also in the expression of *TCF7*⁺ ($p < 0.0001$), CCR7⁺ ($p < 0.0001$), *IL7R*⁺ ($p < 0.0001$). Other genes related to the differentiation of Tregs (*CTLA4*⁺, $p < 0.0001$) or related to cytotoxic CD4⁺ T cells (*NKG7*⁺, *GZMK*⁺, $p = 0.001$ respectively) were found in early stages of differentiation in EBV positive individuals in comparison to EBV negative at the 18 months (Fig. 6C-D and Supplementary Fig. 13). B cells in EBV-seronegative patients showed increased differentiation into B memory and plasmablasts (*BANK1*⁺*MZB1*⁺,*CXCR5*⁺) at 18 months after teplizumab (Fig. 6E-F and Supplementary Fig. 14).

## Discussion

By studying patients at risk for, and with clinical T1D who were treated with teplizumab, we find novel immune modulatory effects of EBV and its synergistic interaction with the anti-CD3 mAb teplizumab. While EBV has been linked to autoimmune diseases, it is often viewed as a target of rather than a modifier of pathologic immune responses. Our hypothesis was that latent EBV might have broad effects on immune cells including antigen specific CD8⁺ T cells. Therefore, we compared immune cells and their responses in individuals who are EBV-seropositive and EBV-seronegative to teplizumab treatment. Before treatment, we identified differences in CD4⁺, CD8⁺, Tregs and B cells in PBMCs from EBV-seropositive vs EBV-seronegative individuals. The expression of genes defining transcriptional pathways were generally decreased which was confirmed by analyzing phosphorylation of ERK in B cells that were triggered by the BCR.

Since the significance of immune modifiers may not be clear under steady state conditions, we analyzed the effects of EBV serostatus when immune cells were disturbed with anti-CD3 mAb. In two independent conducted clinical studies of teplizumab, that enrolled patients with new onset or risk for T1D, there is a more robust clinical effect of the drug in the EBV-seropositive vs seronegative study participants. In addition, in the EBV-seropositive patients, there is an increased frequency of CD8 + T cells that express KLRG1 TIGIT and EOMES which have been associated with partial exhaustion and clinical responses[12]. When we compare the effects of EBV serostatus on the responses to teplizumab over time, we find that there was further inhibition of cell activation pathways which included reduced signaling on $CD4^+$ and $CD8^+$ T cells as well as B cells particularly at the 18 months visit after drug treatment –when the numbers of circulating immune cells are normal. Among antigen specific $CD8^+$ T cells we also identify significant differences in gene expression and pathways of cell activation. Before treatment there are increased expression of IFNγ signaling but after treatment reduced signaling pathways, among them, including TNF and TCR signaling. Because these effects persist after the 14-day treatment with teplizumab, we performed a trajectory analysis that identified different cell differentiation states at the 18 months visit that involved transcription of genes associated with cell cytotoxicity and exhaustion. The expression of TCF7, which is associated with stemness and persistence, is lower on the autoantigen reactive CD8 + T cells from the EBV-seropositive vs seronegative patients who were treated with teplizumab[17–19]. We conclude that latent EBV has broad effects on immune cells and change, altering their differentiation in response to disturbances, potentially influencing pathologic or protective immunity.

Our studies are unique since none previously have studied the effects of EBV in the context of a biologic therapy and because the study participants were relatively young, there was a large proportion of EBV-seronegative patients. Furthermore, we were able to evaluate the effects on immune cells including those antigen specific T cells after teplizumab in the context of the EBV infection.

In a previous study, with another anti-CD3 mAb (otelixizumab), treatment was shown to cause reactivation of latent EBV and there was an increase in the frequency of EBV-reactive $CD8^+$ T cells[20]. This would suggest that the effects of drug treatment were limited to certain T cells and that the exhaustion that we had described was partial. Consistent with the selective and partial effects of the teplizumab treatment, in both AbATE and TN10, in those in whom there was EBV reactivation the viral loads normalized by 8 weeks after treatment. (We cannot, however, exclude that there were increased viral loads that were missed at a different time point or in other tissues such as the nasopharynx or gut where EBV is latent, because of our limited sampling.) We previously showed that teplizumab caused migration of T cells to the gut wall and that the microbiome or immune markers of responses to the microbiome can change the responses to the drug[21,22]. Thus it is possible that the gut wall immune environment, where EBV is latent affects the differentiation of T cells. It is unlikely that the activation only of the EBV-specific $CD8^+$ T cells or even the EBV-reactive $CD4^+$ T cells can account for the improved clinical responses that we found in the two trials or the long-term effects after viral loads had been cleared and had returned to normal. Importantly, our findings do not reflect a non-specific effect of latent DNA viruses on human immune responses since the effects of teplizumab were either absent or the opposite in individuals who were CMV seropositive. This implies there are specific mechanisms associated with EBV latency and more general effects on immune cells that can modulate immune responses.

The effects of EBV are not likely a result of direct viral infection of cells. Among resting memory B cells, the site of EBV latency, the frequency of infected cells has been estimated to be $800/10^6$ cells among immune suppressed patients[23], and EBV is not latent in T cells. The changes in multiple cell populations imply that there are bystander effects and suggests that either soluble mediators may be produced in response to the prior infection and/or that T/B cell interactions are affected. EBV infection has been reported to affect monocyte survival and function, potentially influencing their ability to regulate T and B cell interactions and contributing to the broader immune dysregulation associated with the virus[24–26]. Several mechanisms may be postulated: SoRelle et al described a model in which EBV-infected B cells continuously drives recurrent B cell entry, progression through, and egress from the Germinal Center (GC) reaction creating a perpetual GC. This recurrent cell activation may have effects on both T and B cells and has been associated with features of B cells in autoimmune disorders[27]. BCRF of EBV encodes a viral IL10 homoloque (vIL10), and EBV can lead to human IL-10 production and a decoy vCSF1R, which binds CSF1 and thereby limits mobilization of hemopoietic stem cells[28,29]. The EBV-encoded IL-10 has weaker functionality than cellular IL-10 (cIL-10), but it may be additive or synergistic with cellular IL-10 that is induced by teplizumab, thereby inhibiting cellular immune responses[30]. EBV downregulates Class I MHC and interferes with presentation of viral peptides on Class I and Class II MHC via BDLF3-induced ubiquitination and by BNLF21 by preventing Class I MHC peptide loading by inhibiting the transporter associated with peptide loading (TAP). Interestingly we observed reduced expression of the Class I MHC mediated antigen processing and presentation pathway in the autoantigen T1D specific $CD8^+$ T cells although these cells do not harbor EBV. gP42 can be released in a soluble form which inhibits interaction between Class II MHC and the T cell receptor. The EBV protein, latent membrane protein 2 A (LMP2A), co-opts tyrosine kinases used by the T cell receptor[31,32]. Stable expression of LMP2A in Jurkat T cells down-regulated T cell receptor levels and attenuated T cell receptor signaling. EBV peptides can bind to HLA-E which is a ligand for NKG2A[33]. In previous studies we showed that NKG2A that was induced with teplizumab treatment, served as a ligand for activated $CD8^+$ T cells with regulatory function[34]. In the antigen specific and non-selected memory $CD8^+$ T cells we also found reduced mTOR signaling that has been associated with T cell exhaustion[35]. Although changes in the differentiation of EBV-specific $CD8^+$ T cells based on CD28 and CD27 protein expression have been detected in healthy individuals[36], these markers were not differentially expressed in our transcriptome analysis in the autoantigen specific $CD8^+$ T cells at baseline or after treatment.

In addition to the observed effects on $CD8^+$ T cells we find differences in $CD4^+$ T cells, B cells, and Tregs. The trajectory analysis of $CD4^+$ T cells shows reduced differentiation into memory cells among the EBV-seropositive patients. In addition, the timing of effects of EBV serostatus on cell subsets differed. For some $CD8^+$ T cells there are significant differences before treatment whereas for the others they are detected even 18 months after teplizumab. For $CD4^+$ cells the differences at the baseline best discriminate EBV-seropositive and EBV-seronegative individuals. The changes in B cells are linked in timing to treatment. We do not identify phenotypic differences in the surface expression of IgG or IgM in the EBV-seropositive vs seronegative individuals in samples from another study of teplizumab that were analyzed 12 months after treatment. Collectively, these data indicate that there are systemic immune cell differences in EBV-seropositive vs seronegative individuals with functional consequences that may be identified with an immune perturbant such as teplizumab.

The effects of latent EBV may be influenced by disease specific autoimmune mechanisms. Several autoimmune diseases initiation including MS, Sjogren's syndrome, rheumatoid arthritis, and SLE have been related to EBV infection. Recently, Lanz et al suggest clonally expanded B cells bind EBNA1 and GlialCAM in patients with MS indicating cross reactivity between viral proteins and autoimmune targets[8]. Reduced content and dysfunction of Tregs are closely associated with the occurrence and development of SLE[37]. Additionally, studies by Hong et al and Harly et al highlighted the impact of EBNA2

on chromatin looping interactions and their role in influencing gene expression in multiple autoimmune diseases[38,39]. Collectively these observations add a paradoxical notion to the hygiene hypothesis suggesting that the effects of infectious agents on autoimmune and induced immune responses may differ in a context specific manner. In summary, we have elucidated how prior infection with EBV has broad effects on the immune repertoire and responses to a biologic treatment.

Our findings may have important implications for understanding the development and progression of autoimmune diseases in the context of EBV latency. These findings may also help to develop personalized approaches to immune therapy that consider the biologic activity of the agent in the specific setting of the hosts.

### Limitations of the study

There are limitations to our study. In both trials the frequency of EBV-seropositive and seronegative participants was not equally balanced and there are also more CMV seronegative participants, possibly reflecting the inclusion of pediatric patients who are more frequently seronegative for both viruses. The increasing frequency of EBV-seropositive with age generates a challenge in independently distinguishing the effects of age on metabolic or immunologic findings. However, in the primary analyses of the studies, the age was not a significant determinant of the clinical responses. Conducting further studies with larger numbers of older EBV individuals and more CMV positive individuals would help to clarify this potential confounder. Among the 18 EBV-seropositive individuals treated with teplizumab, 7 were also CMV seropositive and the combined effects of the latent viruses may have influenced the findings with EBV. Additionally, as noted above, we cannot exclude that there may have been reactivation of EBV that was not captured by measuring of viral loads in the study protocols. Given the extended duration of both studies, additional infections with EBV or CMV may have occurred in the seronegative participants during the study course. Importantly, other factors, such as genotypes and additional latent infections, may also influence responses. (We did not find a significant difference in frequency of EBV-seropositive individuals in TN10 participants who were HLA-DR3 negative or positive overall (Fisher's exact test=0.165) or in the teplizumab treated group (Fisher's exact test=0.124). Nonetheless, these unknown factors may be of particular significance in interpreting the transcriptomic data. The scope of the studies and large number of variables renders it impossible to exclude all the potentially contributing factors. Identifying direct relationships between latent viruses and immune responses is challenging due to limited model systems. Human EBV does not infect mice, and mice susceptible to counterparts do not spontaneously develop autoimmune diseases. Consequently, our findings link gene expression differences, but have not directly shown reduced cellular function and impairment in vivo. Because of practical limitations in blood volumes that were available, we cannot perform a direct comparison between the autoantigen specific and the unselected $CD8^+$ T cells to draw conclusions about differential gene expression between these populations. Finally, the studies that were evaluated were relatively small and further investigations with teplizumab or other anti-T cell antibodies are warranted.

## Methods

### Clinical studies

Samples and clinical data were collected from two randomized clinical trials of teplizumab[1,2]. In the TN10 trial (NCT01030861)[1] patients ($n = 76$, 42 males, 34 females) were diagnosed with Stage 2 T1D: They had 2 or more autoantibodies and dysglycemia but did not have clinical T1D (Stage 3). Their median age was 14.0 years (range 8.5-49.1 years). They were randomized to treatment with a single 14-day course of teplizumab ($n = 44$) or placebo ($n = 32$). Participants were monitored at approximately six-month intervals to assess the occurrence of clinical disease (Stage 3 T1D), which was the primary endpoint. The median follow up time was 77 months. Samples for mechanistic studies were collected before treatment and at approximately 3, 6, and 18 months after treatment.

In a second study (AbATE, ITN027AI, NCT00129259)[40] enrolled patients ($n = 77$, 44 males, 33 females) with newly diagnosed Stage 3 T1D ($\leq 8$ weeks). The median age was 12.1 years (range 8.2 to 19.6 years). These patients were randomized to treatment with a 14-day course of teplizumab ($n = 52$) or to an observation group ($n = 25$). A second course of teplizumab was administered to the treatment group at 12 months. Samples were collected at 2-6 months intervals during the 2-year trial.

In both studies, participants underwent screening for EBV (anti-EBV IgG, anti-EBNA, and/or anti-EBV IgM) and CMV (anti-CMV IgG, IgM) at the time of enrollment. EBV and CMV viral copies were also measured during the studies (Table 1). Patients in both studies were excluded if their EBV or CMV viral loads were detectable at the baseline. All patients provided written informed consent or assent. The clinical studies and the use of samples were approved by the IRB's at the study sites[1,40]. All study participants gave written consent or assent for use of their samples for mechanistic studies. Characteristics of PBMCs from individuals selected for scRNAseq or detection of antigen specific cells are specified in Supplementary Data 18. The flow analyses were done on all study participants for whom samples could be acquired. The single cell analysis was done with samples made available from the studies. The investigators were not blinded to the group assignments.

### Metabolic assessments and flow cytometry

In the TN10 trial, the diagnosis of Stage 3 T1D was determined using confirmed responses to an oral glucose tolerance test which was performed approximately every 6 months until the diagnosis of clinical Stage 3 T1D or until the number of events needed for study analysis had occurred. Individuals who had not been diagnosed with Stage 3 T1D at that end of the study were censored. In AbATE, the stimulated C-peptide levels were measured during a 4 h mixed meal tolerance test (MMTT) at baseline, 6, 12, 18, and 24 months. The AUC was calculated and for analysis, transformed (ln (AUC/240 + 1)). The change from the baseline was compared by a mixed model adjusted for age. The group LSMs (95% CI) (i.e. drug or control, EBV-seropositive or seronegative) from the model are shown. OGTT C-peptide and glucose values were tested by Northwest Lipids Research Laboratories using the TOSOH C-peptide immunoassay and Roche glucose assay. EBV serologies were measured at the University of Colorado (TN10) or at ViraCor (AbATE). PBMCs were processed and stored at the NIDDK or ITN repository. Cryopreserved vials of PBMC were sent to ITN Core laboratory at Benaroya Research Institute for analysis by flow cytometry with antibody panels[2,12]. The reagents used for analysis are listed in Supplementary Data 27.

### Single cell RNA sequencing processing and analysis

PBMCs ($25 \times 105$ cells) per patient and visit were reconstituted with wash buffer and incubated with Human TrueStain Fc Blocker (Biolegend) 10 min. TotalSeq antibodies were applied without washing the cells and were incubated at 4 °C for 30 min. After 3 rounds of washing, samples were pooled into one tube based on cell counts, and super-loaded onto the 10× Chromium Chip. The loaded Chip was generated and processed by YCGA (Yale Center for Genome Analysis). The cDNA samples were used to construct 2 types of cDNA libraries, according to the steps outlined in the user guide: gene expression libraries and cell surface hashtag libraries. cDNA libraries were then sequenced on an Illumina Novaseq 6000 platform. The FASTQs were aligned to the human GRCh38 release 91 reference genomes.

### Data processing of raw sequencing reads

Raw sequencing reads were demultiplexed using Cell Ranger mkfastq pipeline to create FASTQ files. Cell Ranger count pipeline (v3.1) was employed in order to perform alignment (using STAR), filtering, barcode counting, and UMI counting. We have used GRCh38 (Ensembl 93) as the genome reference (corresponding to Cell Ranger reference GRCh38-3.0.0).The gene-cell barcode matrices were used for further analysis with the R package Seurat (Seurat development version 4.0.2[41]) with additional utilization of the packages dittoSeq[42], harmony[43], scCustomize, monocle3[16], pheatmap, EnhancedVolcano. Demultiplexing was done using HTODemux with automatic thresholding. Cells were filtered if they were classified as doublets or negative for hashtag antibody based on the demultiplexing results, or if they had fewer than 200 features or greater than 5% mitochondrial RNA was detected.

After removing likely multiplets and low-quality cells, the gene expression levels for each cell were normalized with the NormalizeData function in Seurat followed by the integration of the single cell data. The integrated data was scaled, and the principal analysis was performed. Clusters were identified using FindNeighbors and FindClusters Seurat´s functions. Batch correction was applied using RunHarmony function. Cell cluster identities were manually defined with the cluster-specific marker genes or known marker genes. The cell clusters were visualized using Uniform Manifold Approximation and Projection (UMAP) plots and complete using plot3D. CD8 + , NK, CD4 + , B cells, monocytes and dendritic cells, were re-clustered separately at a resolution between 0.1–0.2 to obtain biologically meaningful clusters each respectively. Subsets functions were used to compare the different types of cells included in the study. A MAST package to run the DE testing implemented in the FindAllMarkers function in Seurat was used to identify up regulated and down regulated genes associated with each individual subset and used for later analysis. To account for donor variability, differentially expressed genes were evaluated for consistency across multiple donors, ensuring that observed transcriptional differences were not driven by a single donor but reflected reproducible patterns across individuals. The identified gene sets were subsequently used for downstream analyses. The DEGs were selected based on p value adjusted after FDR correction ($p < 0.05$). IPA software was used to analyze pathway enrichment. To investigate the kinetics of gene expression during T and B cell differentiation, we performed single-cell trajectory analysis using the Monocle 3 package. The scRNA-seq profiles of CD8 + , CD4+ and B cells were used to reconstruct the single-cell trajectories for the different states. The group-specific marker genes were selected using the graph_test function. We pseudo-temporally ordered the cells using the reduceDimension and orderCells functions. The significance of upregulated expression in the cells was tested by Moran's I test available in graph test function.

### Analysis of autoantigen specific CD8$^{\pm}$ T cells

Peptides representing immunodominant beta cell epitopes were synthesized by Genscript (Piscataway, NJ, USA). HLA-A2 monomers were obtained through the National Institutes of Health (NIH) Tetramer Core Facility (Atlanta, GA, USA). 12 µl of each monomer (0.1 µg/µl) in PBS was multimerised by adding 6 additions 0.6ul of 0.5 mg/ml PE-labelled streptavidin (Thermo Fisher Scientific, Waltham, MA, USA) for 10 min at 4 °C. Multimers were stored at 4 °C and used within 2 weeks.

Freshly thawed PBMCs from baseline and 18 months timepoints were stained with either a pool (0.3 µg each) of HLA-A2 or HLA-A1 combined with HLA-B8 PE labeled tetramers in 200µl T-Cell Media(TCM: RPMI supplemented with 10% human serum, 1% L-Glu, 1% Pen-Strep) at 37 °C for 20 min. Cells were washed with FACS buffer (DPBS,1% BSA, 1 mM EDTA) resuspended in 200ul FACS buffers with 25 µL anti-PE magnetic beads (Miltentyi Biotec) and incubated for 20 min at 4 °C. Cells were washed with FACS buffer, resuspended in 1 mL FACS buffer, a 25 µL Pre-Enriched fraction was reserved and remaining applied to a preequilibrated MACS MS column. The bound cells were washed three times with 0.5 mL FACS buffer, eluted by plunging 2 mL FACS buffer through the column, and centrifuged. The bound (Post) fraction was resuspended in 150 µL FACS buffer, and the flow through was resuspended in 150 µL FACS buffer. Subsequently, cells were stained with a master mix of surface antibodies containing CD8, Dump(CD4, CD14, CD16,CD20, CD40) CD45RA, CCR7, CD161, CD69, CD57, TIGIT, KLRG1 along with the viability dye Sytox Green (1:1000) for 30 min at 4oC. All cells were run on a FACSAria II cell sorter (BD Biosciences, San Jose CA, USA) PE Tetramer+ cell gates were determined by gating on CD8$^{+}$ T in the Pre enriched fraction compared to the flow through. Post enriched tetramer$^{+}$ cells were individually index sorted from the Post tube into 96 well PCR plates using an in scRNAseq platform using Takara Smart-Seq V4 (Takara Bio USA, San Jose, CA, USA) chemistry (Supplementary Fig. 15).

After capture, cells were processed into libraries which were sequenced on a HiSeq2500 sequencer (Illumina, San Diego, CA). The methods for RNA-seq pipeline analysis and TCR clonotype identification are published[44]; differential gene expression analysis was done using DeSeq2 package[45]. The FASTQs were aligned to the human GRCh38 release 91 reference genomes, using STAR v.2.4.2a and gene counts were generated using htseq-count (v0.4.1). Quality control and metrics analysis was performed using the Picard family of tools (v1.134). To identify TCR chains, the Trinity assembler was used to generate contigs. TCR sequences were identified and annotated from these contigs using MiXCR (v2.1.3).

### B cell stimulation and Western blots

B cells were purified with magnetic separation using CD20 microbeads (Miltenyi Biotec). B cells were plated at 100.000 cells/well in a 96-well plate in RPMI/10% FBS and 2.5 µg/ml polyclonal F(ab')2 anti-human IgM (Jackson Immunoresearch).

For Western blot, pre-stimulated purified B-cells were lysed, and proteins extracted using 1X Cell Lysis Buffer (Cell Signaling #9803) supplemented with protease and phosphatase inhibitor cocktail (Thermo Fisher, Cat#78440). A total amount of 10 ug total protein per patient sample was separated by SDS-PAGE and then transferred to a nitrocellulose membrane (Bio-Rad). Signals were detected using SuperSignal West Pico PLUS (Thermo Fisher, Cat#34579) chemiluminescent substrate and imaged using the ChemiDoc XRS+ System (BioRad). Optical density for protein levels was quantified using Image Lab software (BioRad). The primary antibodies and dilutions used for immunoblotting were as follows: pERK1/2, ERK1/2, ERK1/2 and ACTIN Secondary antibody anti-rabbit HRP. Primary and secondary antibodies were from Cell Signaling.

### Assays

Glucose and C-peptides were measured at the Pacific Northwest Lipid Laboratory, Seattle WA, the latter with a TOSOH assay[2,12].

### Statistical analyses

The effects of drug treatment were compared in patients based on their EBV or CMV serostatus at the time of study enrollment. For the survival curves, the rates of conversion from Stage 2 to Stage 3 T1D in the TN10 trial were compared by Log-Rank test with Sidak's adjustment for multiple comparisons.

To compare cell subsets at the baseline by flow cytometry between EBV positive and EBV negative individuals at the baseline, we performed unpaired t tests between the flow parameters in EBV positive and EBV negative. For these comparisons, consistent standard deviations between the groups were assumed. A two stage linear step up following Benjamin, Krieger and Yekutieli method was used to control for false discovery rate (FDR) from multiple hypothesis testing[46].

For analyzing the differences for Fig. 2B and Fig. 3, we employed a mixed-effects linear regression model for repeated measures. For each comparison, the predicted LSMs difference, 95% confidence intervals, and adjusted p-values were calculated and are shown in the graphs with the 95% CI. From the model, the comparisons of EBV serology and treatment are shown. Mixed models were done using SAS 9.4 (Cary, North Carolina) and tests of fixed effects were assessed. The frequency of positive tests for EBV was closely associated with age quartile (Chi-squared $p < 0.0001$ in both trials) and therefore we were unable to adjust for age in mixed models.

A log transformation was applied to the scRNAseq data for improved comprehensibility, as this transformation standardizes the scale and facilitates meaningful comparisons and analysis[47].

### Reporting summary

Further information on research design is available in the Nature Portfolio Reporting Summary linked to this article.

## Data availability

All data are included in the Supplementary Information or available from the authors, as are unique reagents used in this Article. The raw numbers for charts and graphs are available in the Source Data file whenever possible. All sequencing raw and processed data have been deposited in the Gene Expression Omnibus (GEO) database and are publicly available upon publication under the series GSE271063 for the scRNAseq (https://www.ncbi.nlm.nih.gov/geo/query/acc.cgi?acc=GSE271063) and GSE296549 for the bulk RNA seq (https://www.ncbi.nlm.nih.gov/geo/query/acc.cgi?acc=GSE296549). Software is listed in Supplementary Data 27. Data from the AbATE trial are available at ITNTrialShare (www.ITNTrialshare.org) and from the TN10 trial from the NIDDK Data repository. (https://repository.niddk.nih.gov). Source data are provided with this paper.

## References


1. Herold, K. C. et al. Type Diabetes TrialNet Study G. An Anti-CD3 Antibody, Teplizumab, in Relatives at Risk for Type 1 Diabetes. *N. Engl. J. Med.* **381**, 603–613 (2019).
2. Sims, E. K. et al. Type Diabetes TrialNet Study G. Teplizumab improves and stabilizes beta cell function in antibody-positive high-risk individuals. *Sci. Transl. Med.* **13**, (2021).
3. Bjornevik, K. et al. Longitudinal analysis reveals high prevalence of Epstein-Barr virus associated with multiple sclerosis. *Science* **375**, 296–301 (2022).
4. Pender, M. P. et al. Epstein-Barr virus-specific T cell therapy for progressive multiple sclerosis. *JCI insight* **3**, e124714 (2018).
5. Draborg, A. H., Duus, K. & Houen, G. Epstein-barr virus in systemic autoimmune diseases. *Clin. Dev. Immunol.* **2013**, 535738 (2013).
6. Sakkas, L. I., Daoussis, D., Liossis, S.-N. & Bogdanos, D. P. The Infectious Basis of ACPA-Positive Rheumatoid Arthritis. *Front Microbiol* **8**, 1853 (2017).
7. James, J. A. & Robertson, J. M. Lupus and Epstein-Barr. *Curr. Opin. Rheumatol.* **24**, 383–388 (2012).
8. Lanz, T. V. et al. Clonally expanded B cells in multiple sclerosis bind EBV EBNA1 and GlialCAM. *Nature* **603**, 321–327 (2022).
9. Veroni, C. & Aloisi, F. The CD8 T cell-Epstein-Barr virus-B cell trialogue: A central issue in Multiple Sclerosis pathogenesis. *Front. Immunol.* **12**, 665718 (2021).
10. Bach, J.-F. & Chatenoud, L. The hygiene hypothesis: an explanation for the increased frequency of insulin-dependent diabetes. *Cold Spring Harb. Perspect. Med.* **2**, 007799 (2012).
11. Bach, J.-F. The Effect of Infections on Susceptibility to Autoimmune and Allergic Diseases. *N. Engl. J. Med.* **347**, 911–920 (2002).
12. Long, S. A. et al. Partial exhaustion of CD8 T cells and clinical response to teplizumab in new-onset type 1 diabetes. *Sci. Immunol.* **1**, eaai7793 (2016).
13. Perdigoto, A. L. et al. Treatment of type 1 diabetes with teplizumab: clinical and immunological follow-up after 7 years from diagnosis. *Diabetologia* **62**, 655–664 (2019).
14. Long, S. A. et al. Remodeling T cell compartments during anti-CD3 immunotherapy of type 1 diabetes. *Cell Immunol.* **319**, 3–9 (2017).
15. Lledó-Delgado A. et al. Teplizumab induces persistent changes in the antigen-specific repertoire in individuals at-risk for type 1 diabetes. *J. Clin. Invest.* https://doi.org/10.1172/jci177492 (2024).
16. Trapnell, C. et al. The dynamics and regulators of cell fate decisions are revealed by pseudotemporal ordering of single cells. *Nat. Biotechnol.* **32**, 381–386 (2014).
17. Gearty, S. V. et al. An autoimmune stem-like CD8 T cell population drives type 1 diabetes. *Nature* **602**, 156–161 (2022).
18. Abdelsamed, H. A. et al. Beta cell-specific CD8+ T cells maintain stem cell memory-associated epigenetic programs during type 1 diabetes. *Nat. Immunol.* **21**, 578–587 (2020).
19. Escobar G., Mangani D. & Anderson A. C. T cell factor 1: A master regulator of the T cell response in disease. *Sci. Immunol.* **5**, 1–12 (2020).
20. Keymeulen, B. et al. Transient Epstein-Barr virus reactivation in CD3 monoclonal antibody-treated patients. *Blood* **115**, 1145–1155 (2010).
21. Waldron-Lynch, F. et al. Teplizumab induces human gut-tropic regulatory cells in humanized mice and patients. *Sci. Transl. Med.* **4**, 118 (2012).
22. Xie Q. Y. et al. Immune responses to gut bacteria associated with time to diagnosis and clinical response to T cell-directed therapy for type 1 diabetes prevention. *Sci. Transl. Med.* **15** (2023).
23. Babcock, G. J., Decker, L. L., Freeman, R. B. & Thorley-Lawson, D. A. Epstein-barr virus-infected resting memory B cells, not proliferating lymphoblasts, accumulate in the peripheral blood of immunosuppressed patients. *J. Exp. Med.* **190**, 567–576 (1999).
24. Savard, M. et al. Infection of primary human monocytes by Epstein-Barr virus. *J. Virol.* **74**, 2612–2619 (2000).
25. Salek-Ardakani, S., Lyons, S. A. & Arrand, J. R. Epstein-Barr virus promotes human monocyte survival and maturation through a paracrine induction of IFN-alpha. *J. Immunol.* **173**, 321–331 (2004).
26. Tugizov, S. et al. Epstein-Barr virus (EBV)-infected monocytes facilitate dissemination of EBV within the oral mucosal epithelium. *J. Virol.* **81**, 5484–5496 (2007).
27. SoRelle, E. D., Reinoso-Vizcaino, N. M., Horn, G. Q. & Luftig, M. A. Epstein-Barr virus perpetuates B cell germinal center dynamics and generation of autoimmune-associated phenotypes in vitro. *Front. Immunol.* **13**, 1001145 (2022).
28. Houen, G. & Trier, N. H. Epstein-Barr Virus and Systemic Autoimmune Diseases. *Front. Immunol.* **11**, 587380 (2021).
29. Schönrich, G., Abdelaziz, M. O. & Raftery, M. J. Epstein-Barr virus, interleukin-10 and multiple sclerosis: A ménage à trois. *Front Immunol.* **13**, 1028972 (2022).
30. Herold, K. C. et al. Activation of human T cells by FcR nonbinding anti-CD3 mAb, hOKT3gamma1(Ala-Ala). *J. Clin. Invest.* **111**, 409–418 (2003).
31. Ingham, R. J. et al. The Epstein-Barr virus protein, latent membrane protein 2A, Co-opts tyrosine kinases used by the T cell receptor. *J. Biol. Chem.* **280**, 34133–34142 (2005).
32. Ressing, M. E. et al. Interference with T cell receptor-HLA-DR interactions by Epstein-Barr virus gp42 results in reduced T helper cell recognition. *Proc. Natl. Acad. Sci. USA* **100**, 11583–11588 (2003).
33. Mbiribindi, B. et al. Epstein-Barr virus peptides derived from latent cycle proteins alter NKG2A + NK cell effector function. *Sci. Rep.* **10**, 19973 (2020).
34. Ablamunits, V., Henegariu, O., Preston-Hurlburt, P. & Herold, K. C. NKG2A is a marker for acquisition of regulatory function by human CD8+ T cells activated with anti-CD3 antibody. *Eur. J. Immunol.* **41**, 1832–1842 (2011).

35. Chen, Y. et al. Regulation of CD8+ T memory and exhaustion by the mTOR signals. *Cell Mol. Immunol.* **20**, 1023–1039 (2023).
36. Appay, V. et al. Memory CD8+ T cells vary in differentiation phenotype in different persistent virus infections. *Nat. Med.* **8**, 379–385 (2002).
37. Zhu, Y. et al. Regulatory T-cell levels in systemic lupus erythematosus patients: a meta-analysis. *Lupus* **28**, 445–454 (2019).
38. Hong, T. et al. Epstein-Barr virus nuclear antigen 2 extensively rewires the human chromatin landscape at autoimmune risk loci. *Genome Res.* **31**, 2185–2198 (2021).
39. Harley, J. B. et al. Transcription factors operate across disease loci, with EBNA2 implicated in autoimmunity. *Nat. Genet* **50**, 699–707 (2018).
40. Herold, K. C. et al. Teplizumab (Anti-CD3 mAb) treatment preserves C-peptide responses in patients with new-onset type 1 diabetes in a randomized controlled trial: Metabolic and immunologic features at baseline identify a subgroup of responders. *Diabetes* **62**, 3766–3774 (2013).
41. Hao, Y. et al. Dictionary learning for integrative, multimodal and scalable single-cell analysis. *Nat. Biotechnol.* **42**, 293–304 (2024).
42. Bunis, D. G., Andrews, J., Fragiadakis, G. K., Burt, T. D. & Sirota, M. dittoSeq: universal user-friendly single-cell and bulk RNA sequencing visualization toolkit. *Bioinformatics* **36**, 5535–5536 (2021).
43. Korsunsky, I. et al. Fast, sensitive and accurate integration of single-cell data with Harmony. *Nat. Methods* **16**, 1289–1296 (2019).
44. Cerosaletti, K. et al. Single-Cell RNA Sequencing Reveals Expanded Clones of Islet Antigen-Reactive CD4+ T Cells in Peripheral Blood of Subjects with Type 1 Diabetes. *J. Immunol.* **199**, 323–335 (2017).
45. Love, M. I., Huber, W. & Anders, S. Moderated estimation of fold change and dispersion for RNA-seq data with DESeq2. *Genome Biol.* **15**, 550 (2014).
46. Benjamini, Y., Krieger, A. M. & Yekutieli, D. Adaptive linear step-up procedures that control the false discovery rate. *Biometrika* **93**, 491–507 (2006).
47. Butler, A., Hoffman, P., Smibert, P., Papalexi, E. & Satija, R. Integrating single-cell transcriptomic data across different conditions, technologies, and species. *Nat. Biotechnol.* **36**, 411–420 (2018).

## Acknowledgements

KH is a co-inventor on a patent for the use of teplizumab for delay of Type 1 diabetes. Supported by grants DK057846 and AI66387 to KCH. Research reported in this publication was supported by the Core laboratory of the Immune Tolerance Network: National Institute of Allergy and Infectious Diseases of the National Institutes of Health under Award Number UM1AI109565. The content is solely the responsibility of the authors and does not necessarily represent the official views of the National Institutes of Health. We thank the NIH Tetramer Core Facility (contract number 75N93020D00005) for providing HLA Class I monomers for this study.

## Author contributions

Conceptualization: A.L.D, K.C.H., J.M. Data curation: A.L.D, S.A.L., E.J., A.H., H.N., LH, ES, Formal analysis: A.L.D, K.C.H., N.L., L.H., T.S.S., Investigation: A.L.D, P.P-H, K.C.H., Methodology: A.L.D, N.L., EJ, K.C.H., Visualization: A.L.D, K.C.H. Writing original draft: A.L.D., K.C.H., Writing, review and editing: all authors contributed.

## Competing interests

S.A.L. and K.C.H. are listed as a co-inventors for a patent on the use of teplizumab for delay of Type 1 diabetes. K.C.H. has consulted for Sanofi Pharma. The other authors declare no competing interests

## Additional information

**Supplementary information** The online version contains supplementary material available at https://doi.org/10.1038/s41467-025-60276-5.

**Correspondence** and requests for materials should be addressed to Kevan C. Herold.

**Peer review information** *Nature Communications* thanks Richard David Leslie, Christian Münz and the other anonymous reviewer(s) for their contribution to the peer review of this work. A peer review file is available.